Preparation and Performance Analysis of Hydrophobic Composite Membranes with Modified Nano-silica for Construction Applications

Xiaoyan AN *

Hebei Construction Material Vocational and Technical College, Qinhuangdao, 066000, China

http://doi.org/10.5755/j02.ms.39540

Received 25 November 2024; accepted 19 February 2025

In this study, tetraethyl orthosilicate (TEOS) was used as a hydrolysis precursor to prepare nanoscale silica powder and sol through a sol-gel process. Based on the nanosilica (nano-SiO_2) sol, an in-situ modification technique was employed using γ-methacryloxypropyltrimethoxysilane (KH570) and hexadecyltrimethoxysilane (HDTS) as modifiers to obtain modified nano-SiO_2 sol. The modified sol was applied onto glass substrates by manual coating and subsequently cured in a muffle furnace to form a film. The resulting nanocomposite films were characterized by Fourier-transform infrared spectroscopy (FTIR), scanning electron microscopy (SEM), contact angle (CA) measurement, thermogravimetric analysis (TGA), and UV-visible spectroscopy (UV-vis). Analysis of the results indicated that the KH570 and HDTS-modified nano-SiO_2 coatings, due to their large steric hindrance groups, exhibited excellent transparency and hydrophobicity. This modified material shows significant potential for future applications.

Keywords: nano-SiO_2, hydrophobicity, composite film.

1. INTRODUCTION

Nanosilica (nano-SiO_2) is a white, odorless, amorphous powder with a nearly spherical morphology [1]. Its molecular structure typically exhibits a three-dimensional network or chain-like configuration. This material is characterized by its large specific surface area, small particle size, and high stability [2], which lends it to a wide range of applications, including in electromagnetic, medical, construction, petrochemical, and optical fields. Nano-SiO_2's structure contains abundant hydroxyl functional groups, imparting strong hydrophilic characteristics [3]. However, the tendency of hydrogen bonding to promote aggregation limits its compatibility with other materials, necessitating surface modification to enhance dispersibility [4].

Nano-SiO_2 modification is broadly classified into physical and chemical modification techniques [5]. In physical modification, modifiers such as metal oxides or surfactants are physically adsorbed onto the nano-SiO_2 surface [6], which helps reduce intermolecular aggregation and improve the stability of the dispersion. Chemical modification, on the other hand, involves the addition of amine compounds, silane coupling agents, grafted polymers, or alkanol esters to the nano-SiO_2 [7]. This approach leverages nano-SiO_2's hydroxyl groups to chemically react with modifiers, reducing the hydroxyl content and modifying its hydrophilicity or hydrophobicity. Additionally, various functional groups can be grafted onto nano-SiO_2 to endow it with new properties, broadening its application potential [8, 9].

The amine-based modification of nano-SiO_2 exploits the high reactivity of amines to reduce surface hydroxyl groups. Silane coupling agents modify nano-SiO_2 through hydrolysis to form Si-OH groups [10]; one end bonds to the hydroxyl groups on nano-SiO_2 through condensation reactions, forming Si-O-Si linkages, while the other end connects to an organic group, changing the surface from hydrophilic to hydrophobic [11]. This method effectively prevents interparticle aggregation. Grafted polymers incorporate functional groups from long molecular chains with the surface hydroxyl groups of nano-SiO_2, introducing different functionalities [12], while alcohol ester modification alters the surface's wettability via reactions at high temperature and pressure [13].

The sol-gel method is an established technique for synthesizing superhydrophobic coatings and is favored for its simplicity, low cost, and ease of control [14]. The mechanism diagram of coating formation by this method is shown in Fig. 1. Reactive small-molecule precursors undergo rapid hydrolysis to form hydroxyls, resulting in a colloidal solution (sol) and three-dimensional network (gel) structure. The gel is then dried and thermally cured to form nanoporous superhydrophobic surfaces upon solvent removal [15]. By adjusting parameters such as precursor composition and hydrolysis and polycondensation processes, sol-gel films can exhibit varied morphologies and surface energies. This method is compatible with glass, enabling transparent superhydrophobic coatings on glass substrates [16].

Hydrophobic coatings are now widely used, particularly for optical devices such as thin-film solar cells, automotive mirrors, aircraft windshields, and architectural glass. These coatings offer high transparency and excellent self-cleaning capabilities, crucial for applications in diverse environments [17]. Superhydrophobic, transparent optical devices prevent scaling, inhibit bacterial growth, and resist environmental corrosion, thereby enhancing durability and extending the service life of optical equipment.

* Corresponding author. X. An
E-mail: *anxiaoyan@hbjcxy.edu.cn*

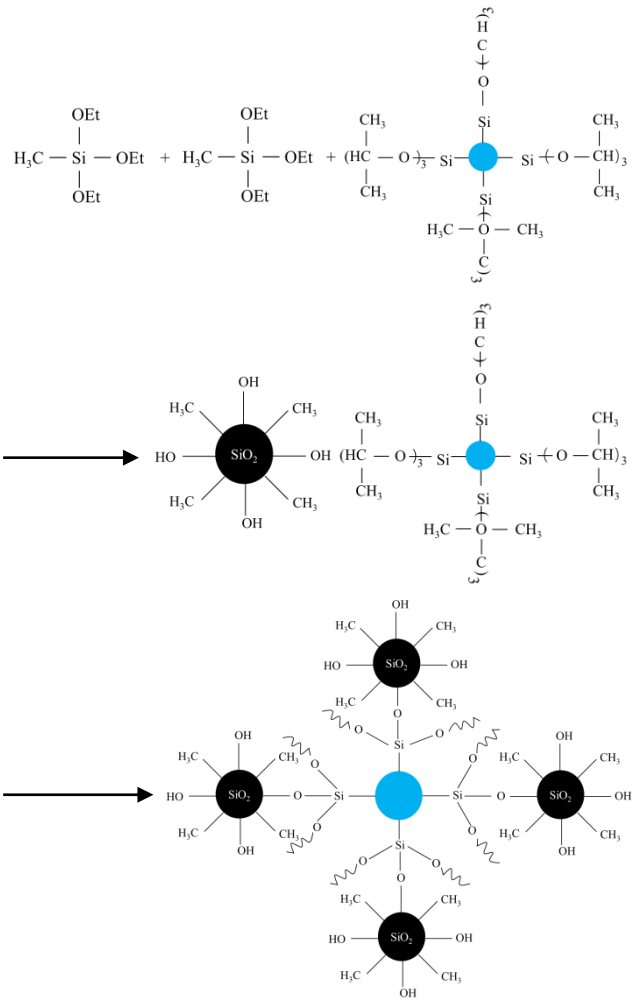

Fig. 1. Schematic diagram of hybrid coating prepared by sol-gel method

In this study, we synthesized nano-SiO_2 powder and sol using tetraethyl orthosilicate (TEOS) as a hydrolysis precursor through the sol-gel method. We modified the nano-SiO_2 sol in situ with γ-methacryloxypropyltrimethoxysilane (KH570) and hexadecyltrimethoxysilane (HDTS). The modified nano-SiO_2 sol was applied manually on a glass substrate, and heating in a muffle furnace was used to form a film. Characterization techniques including Fourier-transform infrared spectroscopy (FTIR), scanning electron microscopy (SEM), contact angle (CA) measurement, thermogravimetric analysis (TGA), and UV-visible spectroscopy (UV-vis) were employed to assess the coatings. The resulting data were analyzed to identify factors influencing the performance of the coatings and to provide theoretical guidance for future product improvements.

2. EXPERIMENT

2.1. Experimental reagents

All chemicals used were of analytical grade. All reagents, including TEOS, anhydrous ethanol (EtOH), 25 wt.% aqueous ammonia, KH570, and HDTS, were purchased from Shanghai Aladdin Biochemical Technology Co., Ltd.

2.2. Experimental equipment

The equipment used includes an electronic balance (JJ600K), a thermostatic convection oven (DCTG-9140A), a scanning electron microscope (Axia ChemiSEM), a UV curing chamber (RAY-400), a laser particle size analyzer (N5), a contact angle goniometer (DAS100), a UV-vis spectrophotometer (UV756C), a thermogravimetric analyzer (Q6000), and a solid-phase in situ thermal infrared detector (Thermolysis/RSFTIR).

2.3. Preparation of materials

First, 22.5 g of TEOS was added to 25 g of deionized water and mixed thoroughly. This mixture was then combined with 25.4 g of anhydrous ethanol. A diluted ammonia solution was added to adjust the pH of the mixture to 9, after which the solution was stirred for 6 hours to complete the hydrolysis reaction, yielding a white, semi-translucent sol. As the sol remained stable without precipitation, centrifugation was used to separate the well-dispersed silica particles, with a centrifuge speed of 15,000 rpm for 30 minutes. The upper solvent layer was removed, and the nano-SiO_2 particles were washed with ethanol. Finally, the particles were dried at a constant temperature of 85 °C for 24 hours in an oven to obtain nano-SiO_2 powder.

The prepared sol was mixed with the modifiers KH570 and HDTS in a 10:1 ratio, respectively. The mixture was then stirred using a magnetic stirrer to ensure complete reaction. The modified hydrophobic sol was subsequently coated onto pre-treated glass slides via spin coating at 2000 rpm for 60 seconds. After coating, the slides were left at room temperature for 2 hours to allow for initial solvent evaporation. The slides were then placed in a muffle furnace and heated gradually at a rate of 2 °C/min until reaching 150 °C, where they were held for 2 hours to fully remove any remaining solvent. This heating process facilitated the complete volatilization of organic compounds, resulting in a rough surface texture on the composite film. The thickness was measured using a thickness gauge, where the thickness of the glass before and after coating was recorded. The average of three measurements was taken, and the coating thickness was calculated based on the difference.

2.4. Characterization methods

The particle size distribution of the nano-SiO_2 sol was measured using a Beckman Coulter N5 laser particle size analyzer with anhydrous ethanol as the dispersing medium. This analyzer measures particle size based on laser scattering, where the spatial distribution of scattered light correlates with particle size and distribution in the sample.

FTIR spectroscopy analysis was performed on the nano-SiO_2 powder using a Vector70 FTIR spectrometer (Bruker, Germany). The scanning range was set from 4000 cm^{-1} to 400 cm^{-1}. Samples were prepared by grinding nano-SiO_2 powder with KBr in a 100:1 mass ratio, followed by pressing the mixture into tablets.

TGA was conducted using a Q5000 TGA (TA Instruments, USA). A sample of 5 – 10 mg was tested, with the temperature ramped from 40 °C to 700 °C at a rate of 10°C/min under a nitrogen atmosphere. Before testing, the sample was thoroughly dried.

The surface morphology of the samples was observed using a high-resolution field-emission scanning electron microscope (Zeiss Merlin, Germany). Samples were cut into 5 mm × 5 mm pieces, affixed onto metal stubs with conductive adhesive, coated with a thin layer of gold for conductivity, and examined in the SEM chamber.

The wettability of the coated surface was evaluated using a DSA100 optical contact angle measurement instrument (KRUSS, Germany). For static contact angle testing, a 4 μL deionized water droplet was dispensed onto the coated surface under stable temperature and humidity conditions. The droplet profile was analyzed with the software to determine the contact angle. Measurements were taken at three different positions on each sample, and the average value was reported.

UV-visible spectral analysis was performed using a UV75SB spectrophotometer (Shanghai Yoke Instruments, China). The transmission properties of the coated glass slides in the UV-visible range (200 – 800 nm) were analyzed by measuring transmission at three different positions on each sample and averaging the results.

3. RESULTS AND DISCUSSION

3.1. SEM characterization

Fig. 2 shows SEM images of cured coatings prepared by spin-coating silica sols modified with KH570 and HDTS agents. As observed in Fig. 2, similar to the unmodified nano-SiO_2 coating, the surface of the KH570-modified sample consists of a combination of micron-sized protrusions and nanoparticles. After modification, the nanoscale SiO_2 particles agglomerate into micron-sized aggregates, resulting in a rough surface with a micro-nano hierarchical structure. The porosity of the coating is relatively low, with an average pore size of approximately 150 nm.

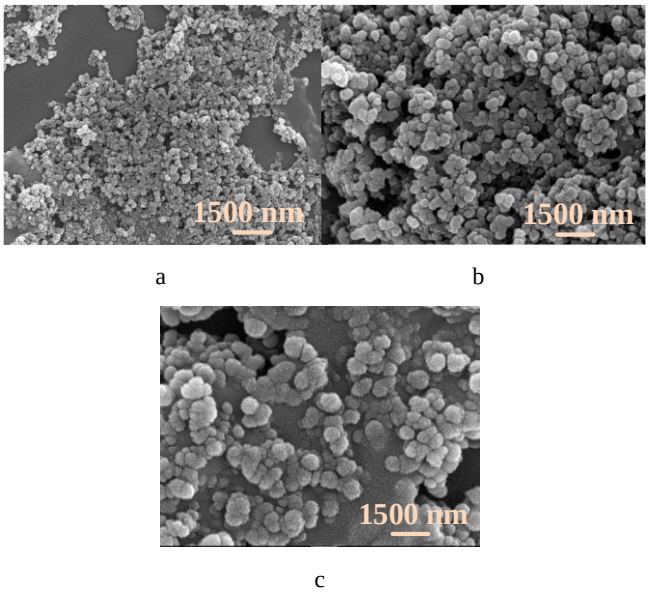

Fig. 2. SEM images of nano-SiO_2 modified coatings: a – nano-SiO_2; b – nano-SiO_2-KH570; c – nano-SiO_2-HDTS

In contrast, the HDTS-modified sample also exhibits a micro-nano rough three-dimensional structure on the surface. However, the coating shows a significantly larger pore size, around 600 nm.

3.2. Effect of different m8odifiers on the particle size of nano-SiO_2 sols

As illustrated in Fig. 3, under identical reaction conditions, the particle size of nano-SiO_2 sols modified by KH570 and HDTS differs. After modification, the average particle size of the unmodified nano-SiO_2 sol is approximately 72 nm, while the KH570-modified sol averages 101 nm, and the HDTS-modified sol averages 122 nm. As the type of modifier changes, the particle size distribution curve shifts progressively rightward, broadening overall. The proportion of particles smaller than 100 nm decreases from 92.1 % to 64.1 % and 46.9 %, respectively.

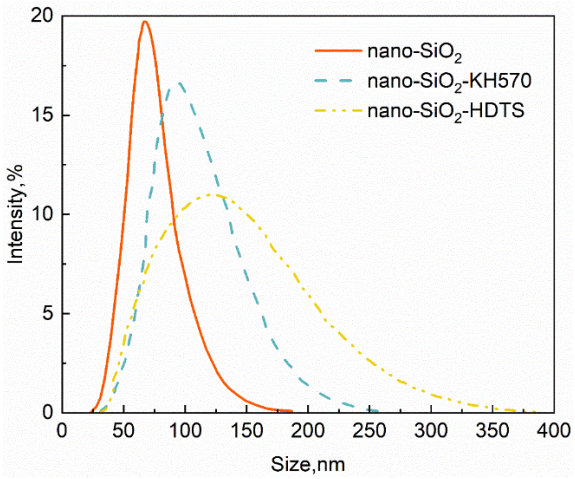

Fig. 3. Influence of modifier type on nano-SiO_2 sol particle size

The analysis indicates that the degree of substitution during the in situ modification process is a crucial factor. For the KH570 modifier, the (3-methacryloyloxy)propyl group presents relatively large steric hindrance, yet it retains some reactivity [18]. As the substitution reaction proceeds, SiO_2 particles undergo further aggregation, forming clusters, which leads to an increase in particle size compared to unmodified nano-SiO_2 sol [19]. Similarly, for the HDTS modifier with a smaller steric hindrance group (-$SiCH=CH_2$), particle aggregation also occurs. However, due to the reduced steric hindrance of the -$SiCH=CH_2$ group, the particle size further increases.

3.3. FTIR analysis of modified nano-SiO_2 powders

The FTIR spectra of the modified nano-SiO_2 powders are shown in Fig. 4, featuring characteristic peaks for siloxane, silanol, structural water, and surface-bound water. In both spectra, characteristic nano-SiO_2 peaks appear, with Si-O-Si bending vibrations at 848 cm^{-1} and 942 cm^{-1} and symmetric stretching vibrations at 1110 cm^{-1}. The broad peak at 3452 cm^{-1} corresponds to -OH symmetric stretching vibrations in structural water, and a peak at 1632 cm^{-1} reflects H-O-H bending vibrations of water. The KH570-modified nano-SiO_2 powder spectrum displays methyl and vinyl stretching vibration peaks around 3400 cm^{-1}, indicating substitution of hydroxyl groups by -Si-$(CH_3)_3$ and -$SiCH=CH_2$ groups. The HDTS-modified powder shows a C=O stretching vibration at 1730 cm^{-1}, indicating that

hydroxyl groups were replaced by (3-methacryloyloxy)propyl groups.

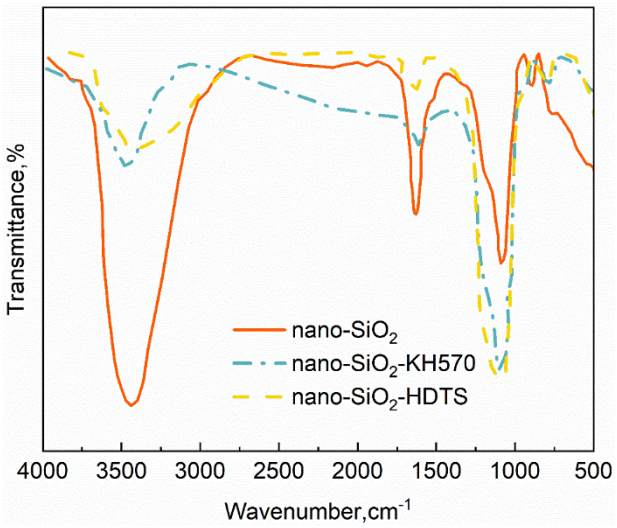

Fig. 4. FTIR spectra of differently modified nano-SiO_2 powders

3.4. TGA of modified nano-SiO_2 powders

To investigate the composition and thermal stability of the differently modified nano-SiO_2 powders, TGA was conducted, and results are shown in Fig. 5. All samples exhibit rapid weight loss below 200 °C. After 200 °C, a slower degradation step is evident in the modified samples. The KH570-modified sample demonstrates a total weight loss of 13.45 %, with a grafting rate of 2.31 % and a secondary decomposition temperature of 415.23 °C. The HDTS-modified sample shows a weight loss of 19.3 %, a grafting rate of 3.33 %, and a secondary decomposition temperature of 392.43 °C.

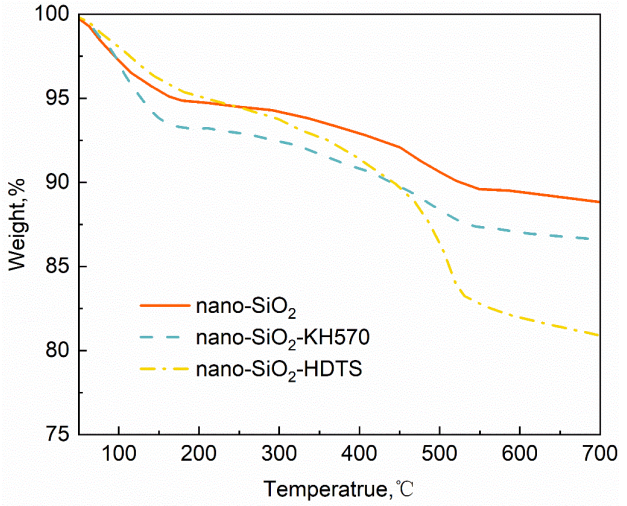

Fig. 5. TGA diagram of modified nano-SiO_2 powder

The analysis suggests that the initial weight loss peak is primarily due to the residual small-molecule substances within the sample. The second weight loss peak is attributed to the oxidation of carbon-containing groups, such as methyl and vinyl groups, present in the modifier [20]. Compared to unmodified nano-silica sol, the final decomposition temperature of the modified nano-silica sol is transparently elevated, indicating that the incorporation of the modifier enhances the thermal stability of the system to some extent. This observation suggests that, during heating, groups within the modifier in the modified nanosilica sol may undergo mutual reactions, potentially resulting in cross-linking, which contributes to the improved thermal stability [21].

3.5. UV-vis spectroscopy

As shown in Fig. 6, the UV-Vis transmittance of the coatings modified by KH570 and HDTS exceeds 85 % in the visible light range of 380 – 780 nm. The measured coating thickness ranges from 20 μm to 40 μm. Specifically, the KH570-modified sample has an average transmittance of about 89.1 %, while the HDTS sample has an average transmittance of about 85.7 %.

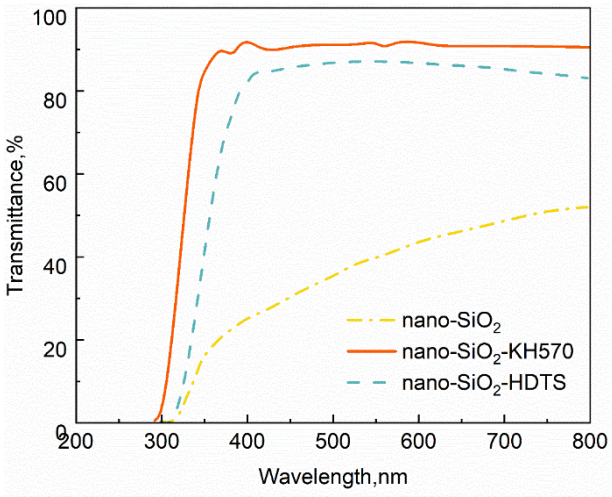

Fig. 6. UV-vis spectrum of samples prepared by direct coating

Analysis indicates that the -OH groups in KH570- and HDTS-modified nano-SiO_2 sols were replaced by -Si-$(CH_3)_3$ and (3-methacryloyloxy)propyl groups with substantial steric hindrance, respectively. This modification reduces particle aggregation during the curing process, enhances dispersion, and results in a coating with excellent transparency.

3.6. Contact angle test of direct coating samples

Contact angle tests were performed on three coatings, and the results are presented in Table 1 and Fig. 7. The contact angles of nano-SiO_2, nano-SiO_2-KH570, and nano-SiO_2-HDTS coatings are 31.6°, 113.5°, and 136.8°, respectively, indicating improved hydrophobicity in the modified samples.

Table 1. Surface contact angle measurements of modified nano-SiO_2 sol coating

Modifier	Surface contact angle, °			Average value, °
nano-SiO_2	31.4	30.9	32.5	31.6
nano-SiO_2-KH570	114.5	112.8	113.2	113.5
nano-SiO_2-HDTS	138.6	136.1	135.6	136.8

This enhancement in hydrophobicity is attributed to the formation of micro-nano rough structures and the replacement of hydrophilic -OH groups with hydrophobic -SiR groups on the modified nano-SiO_2 surface.

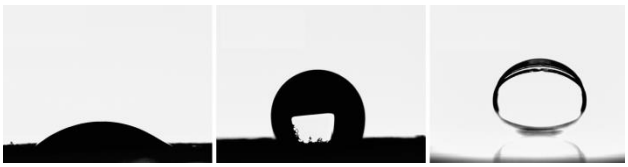

a b c

Fig. 7. Contact angle images of samples prepared by direct coating: a – nano-SiO_2; b – nano-SiO_2-KH570; c – nano-SiO_2-HDTS

4. CONCLUSIONS

1. The KH570- and HDTS-modified nano-SiO_2 coatings possess micro-nano rough three-dimensional structures and reduced porosity.
2. Monodispersed nano-SiO_2 sols with different modifications were successfully synthesized via sol-gel and in-situ modification, exhibiting improved thermal stability. FTIR spectra showing methyl and vinyl stretching peaks around 3400 cm^{-1} and C=O stretching vibration peak at 1730 cm^{-1} confirmed successful synthesis of KH570- and HDTS-modified nano-SiO_2 sols.
3. The modified nano-SiO_2 coatings exhibit excellent transparency, with visible light transmittance reaching 89.1 % and 85.7 % for KH570 and HDTS, respectively. The direct coating method yielded highly transparent films.
4. KH570- and HDTS-modified nano-SiO_2 coatings showed enhanced hydrophobicity with contact angles of 113.5° and 136.8°, respectively, compared to unmodified nano-SiO_2, due to replacement of surface -OH groups with low surface energy groups.

REFERENCES

1. **Murugesan, S., Scheibel, T.** Copolymer/clay Nanocomposites for Biomedical Applications *Advanced Functional Materials* 30 (17) 2020: pp. 1908101. https://doi.org/10.1002/adfm.201908101
2. **Zuo, Y., Zheng, L., Zhao, C., Liu, H.** Micro-/nanostructured Interface for Liquid Manipulation and its Applications *Small* 16 (9) 2020: pp. 1903849. https://doi.org/10.1002/smll.201903849
3. **Zeng, G., Gong, B., Li, Y., Wang, K., Guan, Q.** Nano-silica Modified with Silane and Fluorinated Chemicals to Prepare a Superhydrophobic Coating for Enhancing Self-Cleaning Performance *Water Science & Technology* 90 (3) 2024: pp. 777 – 790. https://doi.org/10.2166/wst.2024.240
4. **Pang, Y., Wang, H., Yang, L., Tang, Q., Li, H., Zhang, J.** Experimental Study on Freeze-thaw Resistance of Mortar: An Attempt to Modify Hydrophobic Materials with Hydrophobic Nano-silica *Journal of Building Engineering* 95 2024: pp. 110152. https://doi.org/10.1016/j.jobe.2024.110152
5. **Zhang, H., Zhou, X., Guo, H., Zhang, Y., Li, D., Ye, F., Tong, Y., Wang, Z.** Effects of Particle Size and Modifier Amount on Hydrophobicity of As-synthesized and Modified Nano-silica Spheres *Ceramics International* 50 (12) 2024: pp. 21511 – 21518. http://doi.org/10.1016/j.ceramint.2024.03.264
6. **Sharma, K., Malik, M.K., Hooda, A., Pandey, K., Sharma, J., Goyat, M.S.** Triethoxyoctylsilane-modified SiO_2 Nanoparticle-based Superhydrophobic Coating for Corrosion Resistance of Mild Steel *Journal of Materials Engineering and Performance* 32 (14) 2023: pp. 6329 – 6338. http://dx.doi.org/10.1007/s11665-022-07580-z
7. **Batool, M., Albargi, H.B., Ahmad, A., Sarwar, Z., Khaliq, Z., Qadir, M.B., Arshad, S.N., Tahir, R., Ali, S., Jalalah, M., Irfan, M., Harraz, F.A.** Nano-Silica Bubbled Structure Based Durable and Flexible Superhydrophobic Electrospun Nanofibrous Membrane for Extensive *Functional Applications Nanomaterials* 13 (7) 2023: pp. 1146. https://doi.org/10.3390/nano13071146
8. **Lucky, A.S., Kumar, P.K.J.P., Kamal, K.K.K.** A Experimental Investigation on Synthesized & Characterized Self-Cleaning Modified Super Hdrophobic Nano-SiO_2 Coating for Solar Photovoltaic Application: Effects of HDTMS & TEA *Indian Journal of Engineering and Materials Sciences (IJEMS)* 30 (4) 2023: pp. 588 – 596. http://doi.org/10.56042/ijems.v30i4.386
9. **Jiang, X., Zhou, C., Su, J., Li, N.** Enhancing Durability of Superhydrophobic Surfaces via Nanoparticle-induced Bipolar Interface Effects and Micro-nano Composite Structures: A Femtosecond Laser and Chemical Modification Approach *Surfaces and Interfaces* 53 2024: pp. 105094. http://doi.org/10.1016/j.surfin.2024.105094
10. **Huang, Y., Zhao, Z., Liu, H., Zou, X., Wang, J.** Two Combination Strategies of Coordinated Silicon Elastomer and Modified Nano-silica to Fabricate Self-healing Hybrid Coating@ Fabrics with High Oil-water Separation Capabilities *Colloids and Surfaces A: Physicochemical and Engineering Aspects* 658 2023: pp. 130685. https://doi.org/10.1016/j.colsurfa.2022.130685
11. **Ghamarpoor, R., Jamshidi, M.** Preparation of Superhydrophobic/Superoleophilic Nitrile Rubber (NBR) Nanocomposites Contained Silanized Nano Silica for Efficient Oil/Water Separation *Separation and Purification Technology* 291 2022: pp. 120854. https://doi.org/10.1016/j.seppur.2022.120854
12. **Ghamarpoor, R., Jamshidi, M.** Silanizing Nano SiO_2 and Its Application in Recycled Nitrile Rubber to Prepare Super Oil Resistant/superhydrophobic/superoleophilic Oil/water Separator *Journal of Environmental Chemical Engineering* 10 (3) 2022: pp. 107971. https://doi.org/10.1016/j.jece.2022.107971
13. **Gong, X., Meng, Y., Zhu, J., Wang, X., Lu, J., Cheng, Y., Tao, Y., Wang, H.** Construct a Stable Super-hydrophobic Surface Through Acetonitrile Extracted Lignin and Nano-silica and its Application in Oil-water Separation *Industrial Crops and Products* 166 2021: pp. 113471. https://doi.org/10.1016/j.indcrop.2021.113471
14. **Ullah, N., Zafar, M., Malik, H., Zaman, K., Raheej, M., Ali, I., Younas, M., Molaei, M.J., Rezakazemi, M.** Fabrication and Characterization of Functionalized Nano-silica Based Transparent Superhydrophobic Surface *Materials Chemistry and Physics* 267 2021: pp. 124694. https://doi.org/10.1016/j.matchemphys.2021.124694
15. **Wang, J., Zhang, L., Li, C.** Superhydrophobic and Mechanically Robust Polysiloxane Composite Coatings Containing Modified Silica Nanoparticles and PS-grafted Halloysite Nanotubes *Chinese Journal of Chemical Engineering* 52 2022: pp. 56 – 65. https://doi.org/10.1016/j.cjche.2021.12.017

16. **She, W., Yang, J., Hong, J., Sun, D., Mu, S., Miao, C.** Superhydrophobic Concrete with Enhanced Mechanical Robustness: Nanohybrid Composites, Strengthen Mechanism and Durability Evaluation *Construction and Building Materials* 247 2020: pp. 118563. https://doi.org/10.1016/j.conbuildmat.2020.118563
17. **Klein, R.J., Maarten Biesheuvel, P., Yu, B.C., Meinhart, C.D., Lange, F.F.** Producing Super-hydrophobic Surfaces with Nano-silica Spheres *International Journal of Materials Research* 94 (4) 2022: pp. 377 – 380. https://doi.org/10.1515/ijmr-2003-0068
18. **Hou, C., Cao, C.** Superhydrophobic Cotton Fabric Membrane Prepared by Fluoropolymers and Modified Nano-SiO_2 Used for Oil/water Separation *RSC Advances* 11 (50) 2021: pp. 31675 – 31687. https://doi.org/10.1039/d1ra06393f
19. **Wang, X., Lin, Z.** Robust, Hydrophobic Anti-corrosion Coating Prepared by PDMS Modified Epoxy Composite with Graphite Nanoplatelets/nano-silica Hybrid Nanofillers *Surface and Coatings Technology* 421 2021: pp. 127440. https://doi.org/10.1016/j.surfcoat.2021.127440
20. **Ismail, A., Saputri, L.N.M.Z., Dwiatmoko, A.A., Susanto, B.H., Nasikin, M.** A Facile Approach to Synthesis of Silica Nanoparticles from Silica Sand and Their Application as Superhydrophobic Material *Journal of Asian Ceramic Societies* 9 (2) 2021: pp. 665 – 672. https://doi.org/10.1080/21870764.2021.1911057
21. **Chen, H., Wang, B., Li, J., Ying, G., Chen, K.** High-strength and Super-hydrophobic Multilayered Paper Based on Nano-silica Coating and Micro-fibrillated Cellulose *Carbohydrate Polymers* 288 2022: pp. 119371. https://doi.org/10.1016/j.carbpol.2022.119371